NANO LETTERS

Letter

pubs.acs.org/NanoLett

Rational Concept for Designing Vapor–Liquid–Solid Growth of Single Crystalline Metal Oxide Nanowires

Annop Klamchuen,[†] Masaru Suzuki,[‡] Kazuki Nagashima,[§] Hideto Yoshida,[†] Masaki Kanai,[§] Fuwei Zhuge,[§] Yong He,[§] Gang Meng,[§] Shoichi Kai,[‡] Seiji Takeda,[†] Tomoji Kawai,[†] and Takeshi Yanagida*[,†,§]

[†]Institute of Scientific and Industrial Research, Osaka University, 8-1 Mihogaoka, Ibaraki, Osaka 567-0047, Japan

[‡]Department of Applied Quantum Physics and Nuclear Engineering, Faculty of Engineering, Kyushu University, 744 Motooka, Nishi-ku, Fukuoka 819-0395, Japan

[§]Institute for Materials Chemistry and Engineering, Kyushu University, 6-1 Kasuga-Koen, Kasuga, Fukuoka 816-8580, Japan

Supporting Information

ABSTRACT: Metal oxide nanowires hold great promise for various device applications due to their unique and robust physical properties in air and/or water and also due to their abundance on Earth. Vapor–liquid–solid (VLS) growth of metal oxide nanowires offers the high controllability of their diameters and spatial positions. In addition, VLS growth has applicability to axial and/or radial heterostructures, which are not attainable by other nanowire growth methods. However, material species available for the VLS growth of metal oxide nanowires are substantially limited even though the variety of material species, which has fascinating physical properties, is the most interesting feature of metal oxides. Here we demonstrate a rational design for the VLS growth of various metal oxide nanowires, based on the "material flux window". This material flux window describes the concept of VLS nanowire growth within a limited material flux range, where nucleation preferentially occurs only at a liquid–solid interface. Although the material flux was previously thought to affect primarily the growth rate, we experimentally and theoretically demonstrate that the material flux is the important experimental variable for the VLS growth of metal oxide nanowires. On the basis of the material flux window concept, we discover novel metal oxide nanowires, composed of MnO, CaO, Sm_2O_3, NiO, and Eu_2O_3, which were previously impossible to form via the VLS route. The newly grown NiO nanowires exhibited stable memristive properties superior to conventional polycrystalline devices due to the single crystallinity. Thus, this VLS design route offers a useful guideline for the discovery of single crystalline nanowires that are composed of functional metal oxide materials.

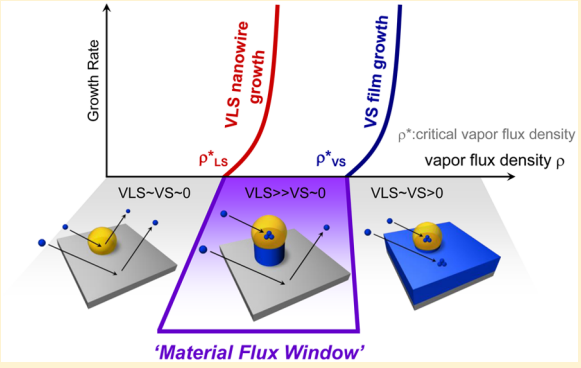

KEYWORDS: *Metal oxide nanowires, vapor–liquid–solid growth, single crystal*

The vapor–liquid–solid (VLS) method has proven to have great potential for the synthesis of well-defined single crystalline nanowires from functional inorganic materials.[1−7] In VLS method, the diameter and spatial nanowire position can be controlled by adjusting the size and spatial position of the metal catalyst. In addition, the heterostructures along the axial or radial directions can be sequentially designed using the VLS process.[8] These unique and fascinating features of the VLS method are not attainable by other nanowire growth methodologies.[9] However, the VLS route for synthesizing nanowires composed of the desired functional materials has been only an approximate and unreliable method. For example, VLS nanowire growth of functional metal oxides, which exhibit unique and robust physical properties, such as photocatalyst activity, high-T_c superconductivity, ferromagnetism, ferroelectricity, and memristive behaviors,[10] has been difficult. Metal oxides whose nanowires can be grown via the VLS route are typically ZnO, SnO_2, In_2O_3, Ga_2O_3, and MgO.[11−14] Because exotic functionalities exist in other metal oxides that include transition metal elements, one exciting and important issue in material chemistry is to overcome the current limitation of the available material species for metal oxide VLS nanowire growth.

The most important phenomenon for VLS nanowire growth is selective crystal growth only at the liquid–solid (LS) interface. Since the discovery of VLS growth of Si whiskers with Au catalysts,[15] numerous experimental and theoretical efforts have been devoted to understanding the intrinsic origin of such spatial selective crystal growth mainly for conventional semiconductor materials, including those from Group IV and III–V.[16,17] Meng et al. have reported the major framework of

Received: April 24, 2015
Revised: August 19, 2015
Published: September 15, 2015

DOI: 10.1021/acs.nanolett.5b01604
Nano Lett. 2015, 15, 6406−6412

nanowire growth in terms of supersaturation.[18] We recently demonstrated via a molecular dynamics (MD) simulation[19] that the VLS growth of compounds requires a difference between the LS interface and vapor−solid (VS) interface for a "critical material flux", above which the nucleation starts to emerge. However, the applicability of this theoretical framework to experimental studies has been substantially limited because there is no clear experimental concept based on this theory and also the effect of material variations has not been considered in the theory. In this study, we propose the "material flux window" experimental concept for designing metal oxide nanowires via the VLS route. This concept suggests that experimentalists find an appropriate material flux range (window) in which the nucleation preferentially occurs at the LS interface to grow the desired metal oxide nanowires via the VLS method, as illustrated in Figure 1. The key physical phenomenon for

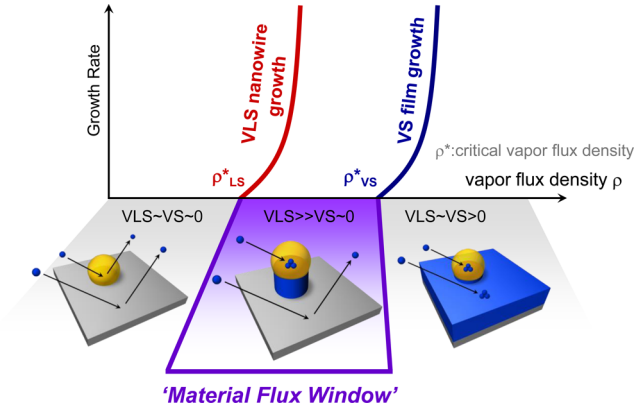

Figure 1. Schematic of the material flux window concept to design a metal oxide nanowire via the VLS route.

obtaining such a material flux window is the interaction between the supplied vapor species and the liquid (catalyst) atoms, which reduces the critical material flux for the nucleation only at the LS interface. Therefore, the critical material flux for VLS nanowire growth should always be lower than the flux for VS film growth. Thus, VLS nanowire growth should occur within the material flux window between the two critical material fluxes of VLS nanowire growth and VS film growth. Although the use of supersaturation is preferred to explain the material dependence for nanowire growth, the values of equilibrium vapor pressure for the most metal oxides were unfortunately unavailable. Therefore, we use the vapor flux density, which is convenient for experimentalists to control. Although the material flux was previously believed to be solely related to the growth rate, this study demonstrates the discovery of novel metal oxide nanowires formed via the VLS route by finding the appropriate material flux window and considering the material dependence on the window.

First, we examine the material flux effects on the metal oxides, whose nanowires are easily formed by VLS, including ZnO, SnO_2, In_2O_3, and MgO. Figure 2 displays both the VLS nanowire growth rate and VS film growth rate when only the supplied metal flux is varied. The growth temperature, oxygen partial pressure, and total pressure are 750 °C, 10^{-2} Pa, and 10 Pa, respectively. The metal targets were employed as the supply sources for these VLS growths. Au catalysts were utilized for the VLS growth, and the other details of the growth experiments are provided in the Methods section and in the Supporting Information S1. Several features can be observed in the experimental data of Figure 2. First, for all materials VLS nanowire growth emerges at a certain metal flux range that is always lower than that required for VS film growth, resulting in a material flux window for VLS regime. These experimental results are consistent with our concept of an appropriate material flux range for the VLS process. Second, a significant material dependence on the material flux window width occurs. We define the material flux window as the flux range between the critical fluxes for VLS nanowire growth and VS film growth.

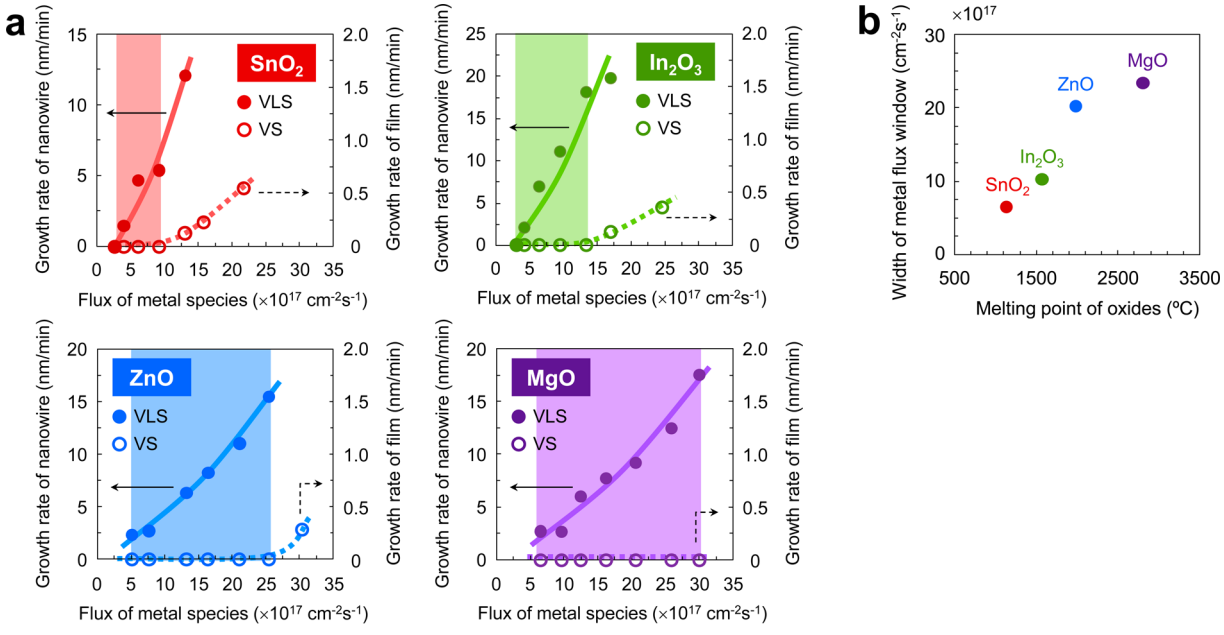

Figure 2. (a) Effect of metal flux on the material flux window of VLS nanowire growth for typical oxides, including SnO_2, In_2O_3, ZnO, and MgO. The growth rates of VLS nanowires and VS thin films were shown in the figures for the comparison. (b) Correlation between the melting point of metal oxides and the material flux window width in the data of panel (a).

DOI: 10.1021/acs.nanolett.5b01604
Nano Lett. 2015, 15, 6406−6412

The material dependence on the material flux window width is MgO > ZnO > In_2O_3 > SnO_2. The same material dependence was also confirmed when the oxygen flux (the oxygen partial pressure) was varied under the constant metal flux, as described in the Supporting Information S2. The fundamental issue is to understand the material dependence on the material flux window width in terms of the material properties. From the viewpoint of their material properties, the material dependence order is consistent with the compound melting points (2852 °C for MgO, 1975 °C for ZnO, 1910 °C for In_2O_3, and 1630 °C for SnO_2),[20] as shown in Figure 2. Because the compound melting point correlates with the bonding strength between elements of compounds, it is essential to understand how the atomic interaction (i.e., the bonding strength) affects the nucleation dynamics during VLS nanowire growth.

It is experimentally difficult to directly observe the effect of bonding strength on VLS nanowire growth. Thus, we performed MD simulations to qualitatively examine the effect of bonding strength on the VLS growth dynamics. The details of the MD simulations for VLS compound growth is described in ref 18 and in the Supporting Information S3. We use previous MD models to calculate both the VLS growth rate and VS film growth rate.[19] Figure 3a displays the calculated data for

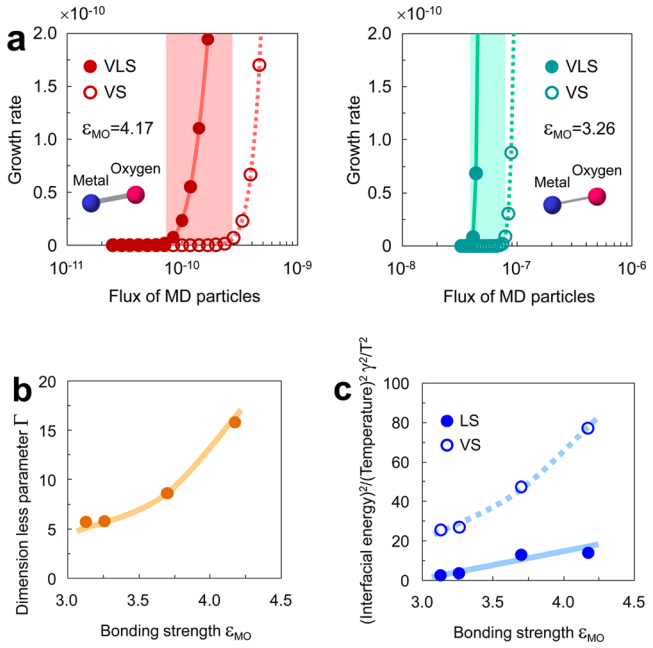

Figure 3. (a) MD calculation data calculated for the VLS nanowire growth rate and VS thin film growth rate when the bonding strength between compound elements was varied. (b) Variation of the dimensionless parameter, Γ, when varying the bonding strength between compound elements. (c) Effect of the bonding strength of compound elements on the interfacial energies at both the VS and LS interfaces.

both the VLS growth rate and VS film growth rate when only the value of the interaction between the metal and oxygen, ε_{MO}, was varied. In the MD simulations, a larger ε_{MO} corresponds to a stronger bonding strength between the metal and oxygen. The MD simulation data demonstrate the presence of a material flux window. The simulation also demonstrates that increasing the value of ε_{MO} widens the material flux window, which is consistent with our experimental trends in Figure 2.

One important issue is clarifying the mechanism of the correlation between the compound bonding strength and material flux window width. Understanding this correlation will be a foundation for tailoring the VLS growth of various metal oxide nanowires. We explore these mechanisms by comparing the MD simulation data with classical nucleation theory. In principle, the material flux window width correlates with the difference between the LS and VS interfaces for the critical material flux required for nucleation. Based on classical nucleation theory, the critical material flux is determined by the activation energy barrier height for nucleation, which is proportional to $(\gamma/T)^2$, where γ is the interfacial energy and T is the temperature.[19] Therefore, the material flux window width is determined by the difference between the two interfaces (LS and VS) for the interfacial energy, that is, $\{(\gamma_{VS}/T)^2 - (\gamma_{LS}/T)^2\}$. To correlate the bonding strength ε_{MO} and the material flux window width in the simulations, we define a dimensionless parameter, Γ, that corresponds to the material flux window width (i.e., a larger Γ corresponds to a wider material flux window). $\Gamma \equiv (\gamma_{VS}^2 - \gamma_{LS}^2)/4(k_BT)^2$, where k_B is the Boltzmann constant. The values of γ_{VS} and γ_{LS} are determined by applying the classic nucleation theory to the MD simulation data.[19] The detailed theoretical descriptions for Γ, γ_{VS}, and γ_{LS} are given in the Supporting Information S3. Figure 3b displays the calculated data for Γ when ε_{MO} is varied, and Figure 3c displays the effect of bonding strength, ε_{MO}, on $(\gamma_{VS}/T)^2$ and $(\gamma_{LS}/T)^2$ for the same data. Increasing ε_{MO} resulted in an increase in Γ values, and in Figure 3c the difference between $(\gamma_{VS}/T)^2$ and $(\gamma_{LS}/T)^2$ increases. The MD simulation data suggest that the compounds with the stronger bonding strength exhibit a wider material flux window by modifying the values of γ_{VS} and γ_{LS}. As shown in Figure 3c, the bonding strength dependence on $(\gamma_{VS}/T)^2$ is stronger than that for $(\gamma_{LS}/T)^2$. Thus, this difference causes the material dependence on the material flux window width. We question why the bonding strength dependence of γ_{VS} is stronger than that for γ_{LS}. On the basis of the definition of interfacial energy,[21] γ_{VS} at the VS interface increases with increasing bonding strength due to the presence of unbound atoms at the solid surfaces. At the LS interface, the presence of surrounding liquid atoms strongly affects the value of γ_{LS} via the interaction between compound atoms and liquid atoms. Such an interaction lowers the value of γ_{LS} compared to that of γ_{VS}, as shown in Figure 3c. Therefore, the influence of the bonding strength, ε_{MO}, on γ_{LS} at the LS interface must always be lower than that on γ_{VS} at the VS interface because of the presence of interactions with liquid atoms. This intrinsic difference between the LS and VS interfaces due to the presence of liquid atoms causes the different bonding strength dependences on the interfacial energy data, as shown in Figure 3c. Thus, increasing the bonding strength can widen the material flux window because of the increased difference between γ_{VS} and γ_{LS}. Because the interfacial energy critically determines the activation energy barrier height for nucleation (i.e., the growth rate), our model, which is based on the effect of bonding strength on the interfacial energies γ_{VS} and γ_{LS}, provides a rigorous qualitative explanation for the material dependence on the material flux window for VLS growth, as shown in Figure 2.

Our experimental concept based on the material flux window highlights the critical importance of precisely controlling the material flux, which was underestimated in previous studies, when fabricating a metal oxide nanowire via the VLS route. Using this concept, we explored novel VLS growths of metal

DOI: 10.1021/acs.nanolett.5b01604
Nano Lett. 2015, 15, 6406−6412

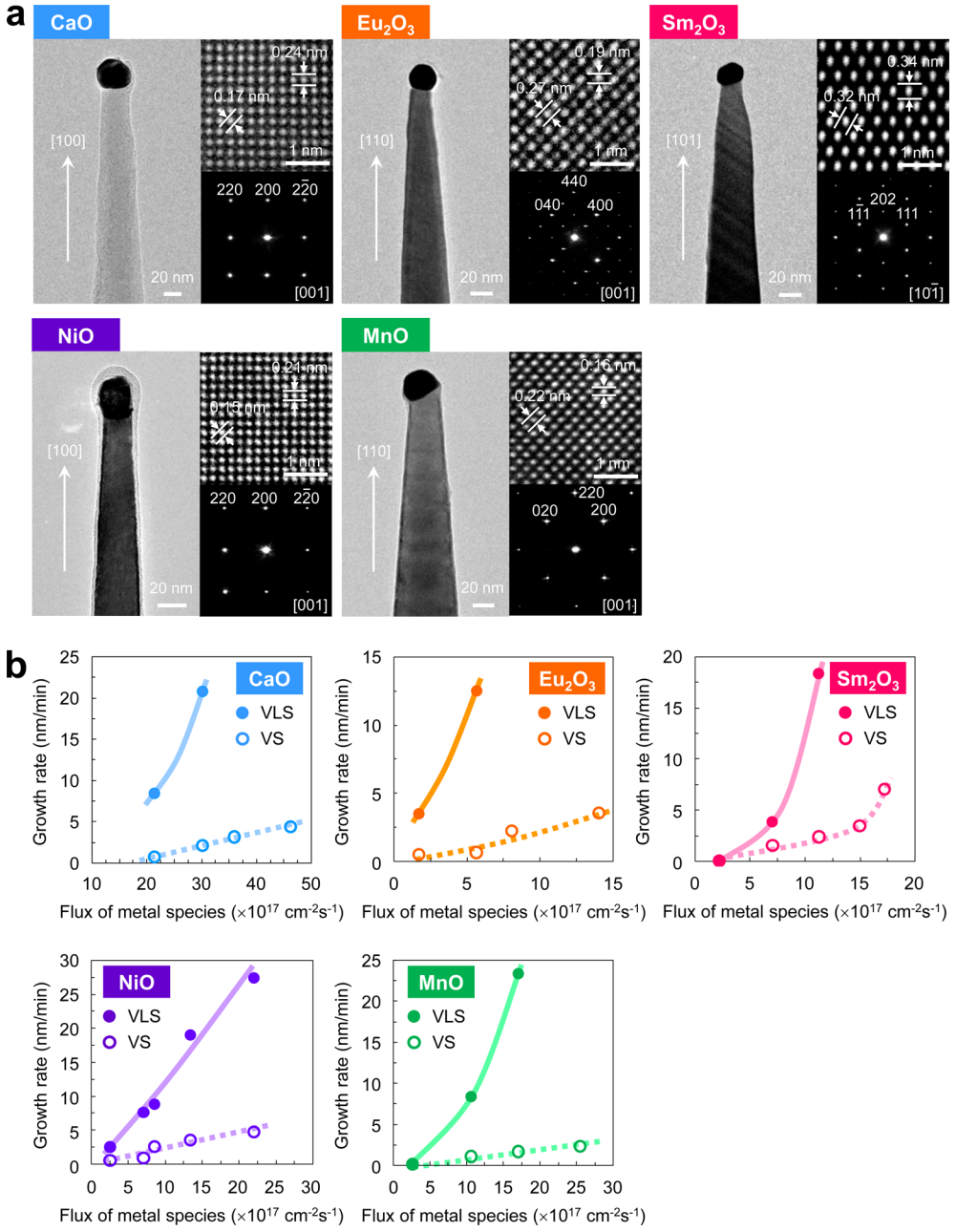

Figure 4. (a) TEM images and SAED data of newly grown metal oxide nanowires via the VLS route (CaO, Eu_2O_3, Sm_2O_3, NiO, and MnO). (b) Effect of metal flux on the VLS nanowire growth rate and VS thin film growth rate of the metal oxides (CaO, Eu_2O_3, Sm_2O_3, NiO, and MnO).

oxide nanowires. Figure 4 displays the transmission electron microscopy (TEM) images of VLS-grown metal oxide nanowires, including MnO, CaO, Sm_2O_3, NiO, and Eu_2O_3, which have not been grown via the VLS route to date. We have chosen these oxides by considering the melting points (1650 °C for MnO, 1990 °C for NiO, 2350 °C for Sm_2O_3, and 2056 °C for Eu_2O_3 and 2580 °C for CaO).[20,21] To create these nanowires by VLS, we performed a strict metal flux control at 850 °C without any intentional oxygen supply, as shown in Figure 4. The metal flux windows for these oxides are narrower than those for conventional VLS oxide nanowire growth, as shown in Figure 2. The narrower material flux windows are observed even when varying the oxygen partial pressures for the oxygen supply, as described in the Supporting Information S4. We did not observe the VLS nanowire growth for MnO, CaO, Sm_2O_3, or Eu_2O_3 when the oxygen gas was intentionally supplied into the chamber (see the data in the Supporting Information Figure S3). Thus, in terms of the material flux window width, there is a significant difference between the VLS nanowire growth of these metal oxides and the conventional VLS nanowire growth of typical metal oxides (MgO, ZnO, In_2O_3, and SnO_2). The major difference is the occurrence of VS film growth. It was difficult to completely suppress VS film growth under the conditions employed in our growth experiments for MnO, CaO, Sm_2O_3, and Eu_2O_3. One possible reason for this difficulty in suppressing VS growth is the use of oxide targets for the material supply. The experiments in Figure 4 utilized oxide targets to supply materials because the metal targets of these materials were not available due to the limitation of the laser ablation process. Because the oxygen supplied from the targets has been found to be significant for VLS growth,[22] our present experimental configurations (Figure

DOI: 10.1021/acs.nanolett.5b01604
Nano Lett. 2015, 15, 6406−6412

4) are not able to completely suppress VS film growth because of the oxygen flux from the target. Thus, the present material flux conditions are slightly above the appropriate material flux window and/or critical material flux for the VS film growth. Therefore, the difference between the material flux dependences (in Figures 2 and 4) is caused by the unintentional oxygen supply from the oxide targets rather than the material flux window variations caused by their material dependences. Because of this extrinsic factor, the direct comparison between these novel VLS oxide nanowires and conventional VLS oxide nanowires is difficult, for example, the comparison on the correlation between the melting points and the material flux window width in Figure 2. Thus, the unintentional oxygen supply can critically affect the VLS growth of metal oxides. In conventional experiments of VLS oxide nanowire growths, it is often difficult to precisely control the oxygen flux in furnaces due to the high residual oxygen partial pressures (in the 10^{-1} Pa range).[24] In the presence of an unintentional oxygen supply, the VLS nanowire growth of metal oxides is difficult for some oxides when their material flux windows exist at a relatively low oxygen partial pressure range (below 10^{-1} Pa). The residual oxygen promotes VS film growth rather than VLS nanowire growth by exceeding the critical material flux for VS film growth. The strict oxygen flux control by using material supply that does not contain oxygen species is the possible solution to suppress the detrimental VS film growth for realizing VLS nanowire growth of metal oxides. Although the material flux control of VLS growth is important, there are several other experimental variables that affect the width and flux values of the material flux window. For example, temperature affects the critical material flux for VS film growth because of the varied equilibrium of the vapor pressure of the solid. Increasing the temperature typically increases the equilibrium vapor pressure and critical material flux value at the VS interface and in some cases at the LS interface. Using different metal catalysts also affects the material flux window due to the different interfacial energy γ_{LS}, as described in the Supporting Information S3. In principle, strengthening the atomic interaction between the catalysts and supplied vapor species widens the material flux window due to the increased difference between γ_{VS} and γ_{LS}. Thus, our present results highlight that it is now possible to design novel functional metal oxide nanowires via the VLS route by finding the appropriate material flux range based on the concept of the material flux window.

The availability of various metal oxide nanowires allows us to explore unique properties of metal oxides within nanowires. As an example, we investigate the memristive devices composed of newly grown NiO single crystalline nanowire. Figure 5 shows the SEM image of single NiO nanowire memristor device on Si substrate. Figure 5b–d shows the memristive data of fabricated NiO nanowire devices. For comparison, the data of polycrystalline memristive devices were shown. The fabrication details of these memristive devices are seen in the Experimental Section. As seen in Figure 5b, the fabricated nanowire device exhibited the bipolar memristive behaviors. Interestingly, the memristive properties of this single crystalline NiO nanowire, including the retention time (Figure 5c) and the statistical distribution of memristive switching voltage (Figure 5d), were found to be superior to those of polycrystalline memristive devices. The longer retention time and the narrower distribution of switching voltage were found for the single crystalline NiO nanowire device. Because the grain boundaries are known to affect the memristive properties via redox events, the present

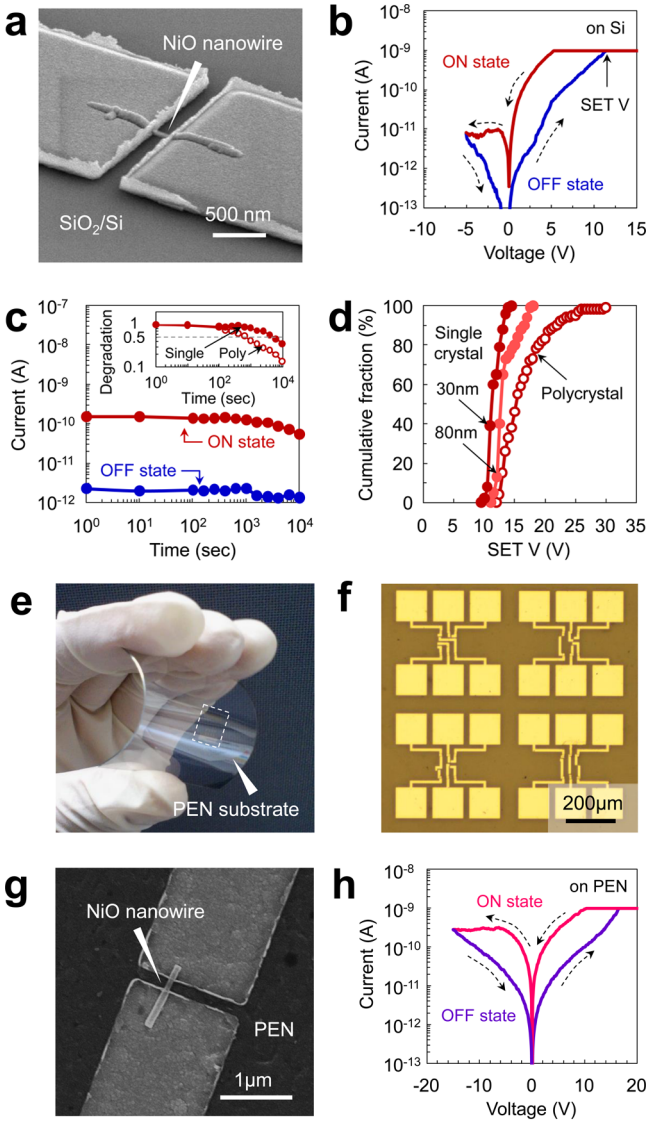

Figure 5. (a) SEM image of fabricated NiO nanowire memristor device on Si substrate. (b) Memristive (I–V) data of NiO memristive device. (c) Retention data of ON state and OFF state, and the inset shows the comparison between NiO single cryctalline nanowire device and NiO polycrystalline device on the retention data of ON state. (d) Distribution data of SET voltage for single crystalline NiO nanowire devices and polycrystalline NiO device. (e,f) Photographs of single crystalline NiO nanowire memristive device on PEN substrate. (g) SEM image of single crystalline NiO nanowire memristive device on PEN substrate. (h) Memristive (I–V) data of single crystalline NiO nanowire memristive device on PEN substrate.

superior memristive properties of nanowire memristor should be the features of single crystalline devices. Furthermore, we fabricated the memristor comprised of single crystalline NiO nanowires onto flexible polyethylene naphthalate (PEN) substrate, as shown in Figure 5e–h. The occurrence of bipolar memristive behavior can be seen. Because conventional techniques using lithography cannot fabricate the single crystalline memristive device on polymer substrates due to the limitations of process temperature and/or epitaxial crystal growth, the present approach using single crystalline NiO nanowires offers stable memristive devices on any substrates. The availability of various single crystalline metal oxide nanowires will open up new research avenues not only for

DOI: 10.1021/acs.nanolett.5b01604
Nano Lett. 2015, 15, 6406–6412

the fundamental study of physical properties in nanoscale metal oxides but also for novel engineering applications by utilizing the unique and robust properties of metal oxides.

In summary, we demonstrate a rational material flux window concept for the design of metal oxide nanowires via the VLS route. Although the material flux was previously believed to affect the growth rate, we experimentally and theoretically demonstrate that the material flux is the most important experimental variable for the VLS growth of metal oxide nanowires. We demonstrate that the material flux windows for conventional oxide nanowires grown via VLS, including ZnO, SnO_2, In_2O_3, and MgO, can be interpreted in terms of the bonding strength between compound elements. On the basis of the material flux window concept, we discover novel metal oxide nanowires that were previously impossible to grow via the VLS route. The newly grown single crystalline NiO nanowires can be utilized as the stable memristive devices on polymer substrate, which has been difficult by conventional fabrication techniques. Thus, this new concept is useful for the design and discovery of novel nanowires that are composed of desirable functional oxide materials.

Experimental Section. Metal oxide nanowires were synthesized by the pulsed laser deposition (PLD) method, as described previously.[23−25] ZnO, In_2O_3, SnO_2, MnO, and Eu_2O_3 nanowires were grown on a sapphire Al_2O_3 (110) substrate, and MgO, CaO, NiO, and Sm_2O_3 nanowires were grown on a MgO (100) substrate (Crystal Base Co. Ltd.). Before nanowire growth, a Au thin layer (∼1 nm) was deposited onto a substrate by direct current (dc) sputtering. Metal tablets or metal oxide tablets (purity over 99.99%; Koujundo Chemicals Co. Ltd.) were utilized to supply the vapor source of material species. Metal targets were used for ZnO, In_2O_3, SnO_2, and MgO nanowire growths, whereas oxide targets were employed for MnO, Eu_2O_3, NiO, CaO, and Sm_2O_3. Laser ablations were performed on the target by utilizing an ArF excimer laser (λ = 193 nm). The ablation area and frequency were 0.02 cm^2 and 10 Hz, respectively, and the laser energy was altered from 40 to 80 mJ to vary the material flux. The oxygen flux was varied by changing the oxygen partial pressure (ranging from 10^{-6} to 10 Pa) in the mixed O_2 and Ar gas to preserve a constant total pressure of 10 Pa. The use of a constant total pressure is important to maintain a constant material transport from the target to the substrate. The typical growth time for the nanowire was 90 min, and the substrate was heated to the desired temperature for the depositions. After nanowire growth, the substrate temperature was cooled to room temperature within 30 min. The nanowire surface morphology was evaluated by field-emission scanning electron microscopy (JEOL, JSM-7001F) at an acceleration voltage of 30 kV. The crystalline structure, composition, and element mapping of the nanowires were analyzed by scanning transmission electron microscopy (STEM, JEOL, JEM-ARM200F) with integrated energy dispersive spectroscopy (EDS) at an acceleration voltage of 200 kV. A Cu mesh covered with a C film was used to support the nanowire samples for the TEM measurements. Selected area electron diffraction (SAED) was performed to analyze the crystal structure. The probe size was approximately 0.19 nm. To quantitatively examine the material flux of the metal species, film depositions at room temperature were carried out under various laser ablation conditions in an Ar atmosphere because the re-evaporation events at the substrate surface were negligible under the low-temperature conditions. After measuring the thickness of the obtained thin film using a surface profiler (Alpha-Step IQ), the material flux was estimated using the density of the element. Memristive devices using NiO nanowires were fabricated onto SiO_2/Si substrate and polyethylene naphthalate (PEN) substrate by 30 kV electron beam (EB) lithography technique. For the SiO_2/Si substrate, 300 nm thick SiO_2 was formed on the degenerated n-type Si (100) substrate (resistivity ∼1−10Ωcm) by thermal annealing. EB lithography process was performed by utilizing a resist ZEP520A-7 (ZEON Corp.). EB lithography for PEN substrate was carried out by using Cr sacrifice conductive layer. Prior to coating the EB resist, 15 nm Cr was sputtered on PEN substrate. After the EB process, the Cr layer was removed by the following etchant, $(NH4)_2[Ce(NO_3)_6]/HClO_4/H_2O$ = 3:1:16. For the electrical contact, Pt electrode was sputtered by using RF magnetron sputtering. The thickness of Pt electrode was ca. 150 nm. Finally the EB resist was lifted-off by *N*,*N*-dimethylformamide (DMF) followed by the cleaning in acetone. The polycrystalline NiO memristive devices were fabricated by combining EB lithography and pulsed laser deposition (PLD) method. First, the line patterns with 100 nm width and 3 μm length were created onto SiO_2/Si substrate by the EB lithography. Then NiO polycrystalline film with the thickness of 100 nm was deposited by ablating a NiO tablet (99.9% pure) using ArF excimer laser (Lamda Physic COMPex 102, λ = 193 nm). The deposition was carried out at room temperature with the oxygen pressure of 10^{-1} Pa. The laser energy, the repetition rate, the substrate−target distance, and the growth rate were 40 mJ, 10 Hz, 45 mm, and 0.6 nm/min. Then the polycrystalline NiO nanobeam was obtained by removing the resist, which was followed by the postannealing process at 300 °C in 10^{-1} Pa oxygen pressure for 90 min. All electrical transport measurements using these nanowire devices were carried out by using Keithley 4200SCS at room temperature in atmospheric condition.

■ ASSOCIATED CONTENT

Supporting Information

The Supporting Information is available free of charge on the ACS Publications website at DOI: 10.1021/acs.nanolett.5b01604.

Detailed descriptions as to fabricating nanowires and devices. Theoretical details for the MD simulations. Effect of oxygen partial pressure on the material flux window width for VLS nanowire growths of MgO, ZnO, In_2O_3, and SnO_2. Effect of oxygen partial pressure on the VLS nanowire growth and VS film growth of MnO, CaO, Sm_2O_3, NiO, and Eu_2O_3. (PDF)

■ AUTHOR INFORMATION

Corresponding Author

*E-mail: yanagida@cm.kyushu-u.ac.jp. Tel.: +81-92-583-8835. Fax: +81-92-583-8820.

Author Contributions

The manuscript was written through contributions of all authors. All authors have given approval to the final version of the manuscript.

Funding

This work was supported by NEXT Project.

Notes

The authors declare no competing financial interest.

DOI: 10.1021/acs.nanolett.5b01604
Nano Lett. 2015, 15, 6406−6412

REFERENCES

(1) Huang, M.; et al. Room-temperature ultraviolet nanowire nanolasers. *Science* **2001**, *292*, 1897−1899.
(2) Hwang, Y. J.; Boukai, A.; Yang, P. High density n-Si/n-TiO_2 core/shell nanowire arrays with enhanced photoactivity. *Nano Lett.* **2009**, *9*, 410−415.
(3) Nagashima, K.; et al. Resistive switching multistate non-volatile memory effects in a single cobalt oxide nanowire. *Nano Lett.* **2010**, *10*, 1359−1363.
(4) Dai, Z. R.; Pan, Z. W.; Wang, Z. L. Novel nanostructures of functional oxides synthesized by thermal evaporation. *Adv. Funct. Mater.* **2003**, *13*, 9−24.
(5) Hochbaum, A. I.; He, R.; Fan, R.; Yang, P. Controlled growth of Si nanowire arrays for device integration. *Nano Lett.* **2005**, *5*, 457−460.
(6) Persson, A. I.; et al. Solid-phase diffusion mechanism for GaAs nanowire growth. *Nat. Mater.* **2004**, *3*, 677−681.
(7) Lee, S. H.; Jung, Y.; Agarwal, R. Highly-scalable Nonvolatile and Ultra-low Power Phase-change Nanowire Memory. *Nat. Nanotechnol.* **2007**, *2*, 626−630.
(8) Lauhon, L. J.; Gudiksen, M. S.; Lieber, C. M. Semiconductor nanowire heterostructures. *Philos. Trans. R. Soc., A* **2004**, *362*, 1247−1260.
(9) Comini, E.; et al. Quasi-one dimensional metal oxide semiconductors: Preparation, characterization and application as chemical sensors. *Prog. Mater. Sci.* **2009**, *54*, 1−67.
(10) Hwang, H. Y.; et al. Emergent phenomena at oxide interfaces. *Nat. Mater.* **2012**, *11*, 103−113.
(11) Yanagida, T.; et al. Enhancement of oxide VLS growth by carbon on substrate surface. *J. Phys. Chem. C* **2008**, *112*, 18923−18926.
(12) Auer, E.; et al. Ultrafast VLS growth of epitaxial β-Ga_2O_3 nanowires. *Nanotechnology* **2009**, *20*, 434017.
(13) Yanagida, T.; Nagashima, K.; Tanaka, H.; Kawai, T. Mechanism of catalyst diffusion on magnesium oxide nanowire growth. *Appl. Phys. Lett.* **2007**, *91*, 061502.
(14) Klamchuen, A.; et al. Study on transport pathway in oxide nanowire growth by using spacing-controlled regular array. *Appl. Phys. Lett.* **2011**, *99*, 193105.
(15) Wagner, R. S.; Ellis, W. C. Vapor-Liquid-Solid Mechanism of Single Crystal Growth. *Appl. Phys. Lett.* **1964**, *4*, 89.
(16) Hannon, J. B.; Kodambaka, S.; Ross, F. M.; Tromp, R. M. The influence of the surface migration of gold on the growth of silicon nanowires. *Nature* **2006**, *440*, 69−71.
(17) Kodambaka, S.; Tersoff, J.; Reuter, M. C.; Ross, F. M. Diameter-Independent Kinetics in the Vapor-Liquid-Solid Growth of Si Nanowires. *Phys. Rev. Lett.* **2006**, *96*, 096105.
(18) Meng, F.; Morin, S. A.; Forticaux, A.; Jin, S. Screw Dislocation Driven Growth of Nanomaterials. *Acc. Chem. Res.* **2013**, *46*, 1616.
(19) Suzuki, M.; et al. Essential role of catalyst in vapor-liquid-solid growth of compounds. *Phys. Rev. E* **2011**, *83*, 061606.
(20) Schneider, S. J. *Compilation of the Melting Points of the Metal Oxides*; U.S. Department of Commerce; National Bureau of Standards: Washington, DC, 1963.
(21) Moore, W. J. *Physical Chemistry* 3rd ed.; Prentice Hall Press: New York, 1962.
(22) Klamchuen, A.; et al. Role of surrounding oxygen on oxide nanowire growth. *Appl. Phys. Lett.* **2010**, *97*, 073114.
(23) Oka, K.; Yanagida, T.; Nagashima, K.; Tanaka, H.; Kawai, T. Non-volatile bipolar resistive memory switching in single crystalline NiO heterostructured nanowires. *J. Am. Chem. Soc.* **2009**, *131*, 3434−3435.
(24) Oka, K.; et al. Resistive switching memory effects of NiO nanowire/metal junctions. *J. Am. Chem. Soc.* **2010**, *132*, 6634−6635.
(25) Nagashima, K.; et al. Intrinsic mechanisms of memristive switching. *Nano Lett.* **2011**, *11*, 2114−2118.

DOI: 10.1021/acs.nanolett.5b01604
Nano Lett. 2015, 15, 6406−6412